Moaz Eldeeb[1,*], Ali Demir[2]

Optimising the Production Process of Rieter Air Jet Spun Yarns and a Model for Prediction of their Strength

DOI: 10.5604/01.3001.0010.7794

[1] **Technical University of Liberec, Department of Textile Technology, Faculty of Textile Engineering,** Liberec, Czech Republic
* E-mail: eldeeb.moaaz@gmail.com

[2] **Istanbul Technical University, Department of Textile Engineering, Faculty of Textile Technologies and Design,** Istanbul, Turkey

Abstract
In this study, the effect of yarn linear density, delivery speed and nozzle pressure on Rieter air jet spun yarn strength was investigated. A multiple regression model was used to study the combined effect of these parameters and response surfaces were obtained. Results showed that by increasing the nozzle pressure, the yarn tensile strength improves till a specific limit, then it deteriorates afterwards. Based on the different combinations of processing variables, optimal running conditions were obtained. Along with the experiment, a mathematical model that predicts air jet spun yarn strength at a short gauge length has been presented. Fibre parameters in addition to yarn structural parameters were used to obtain the theoretical yarn strength. The results showed a satisfactory agreement between the experimental and theoretical results.

Key words: *air jet spinning, linear density, strength, nozzle pressure, delivery speed, prediction, structure.*

Introduction

The air jet spinning process has just reached an industrial acceptance stage, having developed through almost half a century. Known as fasciated spinning, air jet spinning was first introduced by the DuPont Company in 1971 using the principle of air vortices to form a yarn, followed by Murata jet spinning "MJS" in 1982, which consists of two jets rotating in opposite directions. Murata later introduced an improved version of MJS called "MVS" – Murata Vortex Spinning in 1997. The MVS system uses a single nozzle with an inner needle, and this system is now able to produce 100% carded cotton yarns [1, 2].

In 2009, Rieter presented the latest method in air jet spun yarn production. Both the Rieter and MVS systems are based on a similar principle, but the nozzle block in the Rieter system does not contain a needle holder that works as a twisting guide [3]. In this system, as shown in ***Figure 1***, the drafted fibre strand is fed to the vortex chamber, and the channel where the yarn is withdrawn from lies above the fibre feed channel. Therefore during the fibre transport process, some fibres are separated from the main stream, which is approximately straight from the drafting zone to the spindle tube entrance point. Due to the air vortices inside the spindle, these fibres are twisted to wrap around the main fibre strand which forms the yarn core, which is then taken up by the winding device [4]. The air jet spun yarn structure consists of core fibres, which are parallel and consolidating wrapper fibres that lie inclined to the yarn axis at differing angles.

Experimental investigations were carried out on the influence of air jet spinning machine production parameters on yarn properties in order to optimise yarn quality. These parameters are the nozzle (pressure and orifice angle), the distance between the spindle and front roller nip point, the draft, spindle (cross-section, working period and diameter), yarn (linear density and delivery speed) and fibre composition [5-9]. Most of these parameters proved to have a significant effect on final yarn properties. Coarser MVS yarns exhibit superior yarn properties in terms of yarn tenacity, and the nozzle pressure required is higher when spinning these yarns.

Earlier studies carried out on MVS yarn showed that tensile energy initially increases with an increase in nozzle pressure and then deteriorates with any further increase in nozzle pressure. The structural integrity, tensile properties, and abrasion resistance deteriorate at high yarn delivery speeds [10-14]. In this research, some parameters were investigated using this new Rieter air jet spinning technology, namely, yarn linear density, nozzle pressure, and delivery speed. These parameters were proven to influence the fibre configuration and yarn structure significantly. Although these parameters have been investigated, slight differences in nozzle design for both the Rieter and MVS systems may lead to a different trend. Therefore this study aimed to give a good understanding of this new technique.

Along with an experimental study, a mathematical model was established based on an earlier model available in

the literature that predicts air jet spun yarn strength. To achieve the best air jet yarn quality, this necessitates knowing the relationship between fibre properties, yarn structure and yarn properties, which can demonstrate which factor is more important. Furthermore it indicates the limits of each factor. Mathematical models are usually used to describe and explain such relationships. Numerous researchers have made a good contribution to this topic, many of whom presented mathematical models for ring-spun yarns [15-19] and rotor yarns [20]. Nevertheless mathematical models of air jet spun yarns are limited [21, 22]. Rajamanickam et al. presented mathematical models that predict air jet yarn strength. They also obtained a mathematical relationship between the yarn's breaking load and its structure. The model also classified the modes of yarn failure into noncatastrophic (due to partial fibre slippage or breakage at the point of yarn failure) and catastrophic (due to complete fibre slippage or breakage at the point of yarn failure) [23, 24]. However, they obtained a prediction error which was quite high. In this article, their model has been modified to target better prediction accuracy.

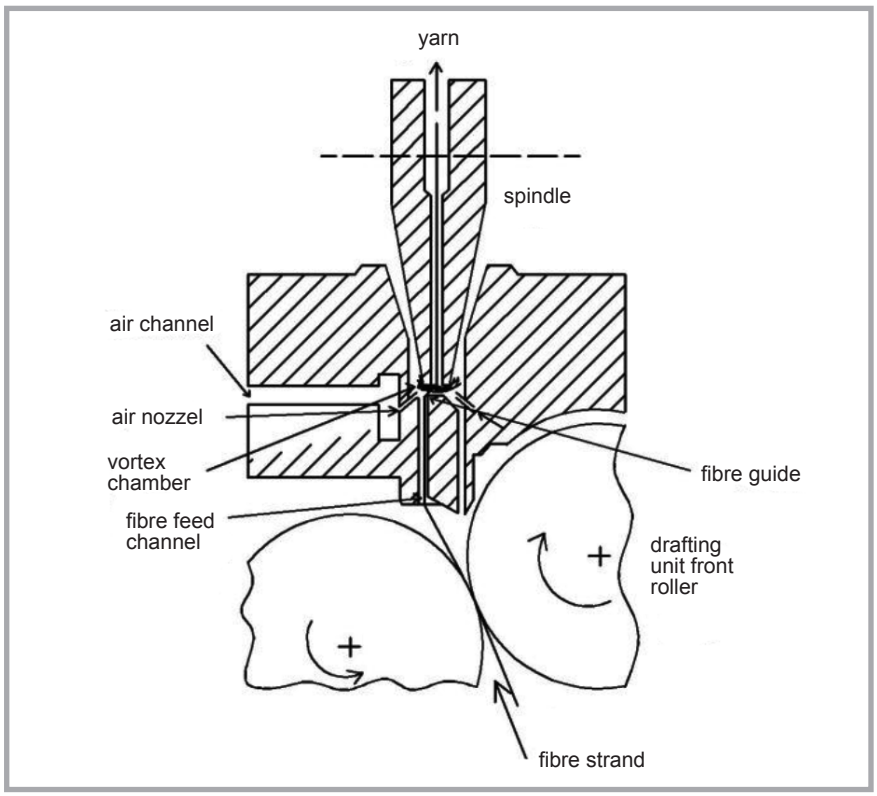

Figure 1. *Schematic diagram of the yarn formation zone on a Rieter air jet spinning machine (adapted and reproduced [4]).*

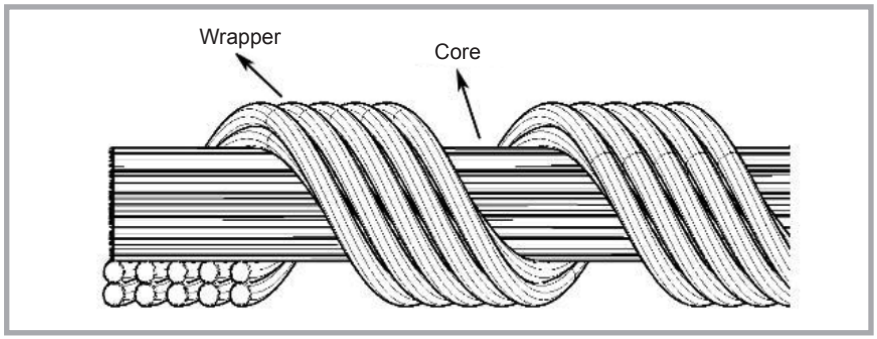

Figure 2. *Simplified model of short staple air jet spun yarn.*

Material and method

100% Viscose fibres (38 mm) were spun to produce air jet spun yarns. After the carding process, the sliver was drawn using three consecutive drawing passages in order to enhance fibre orientation and sliver evenness. The sliver of 3.5 ktex drawn was spun using a Rieter air jet spinning machine J20 (Switzerland) to produce yarns with different counts and machine parameters. The Box-Behnken factorial experimental design is an efficient method to reduce the number of experiments required to study the parameters and their combined effect, and in our study it was used to obtain the combination of yarn count, delivery speed and nozzle pressure. ***Table 1*** shows the parameters chosen and their values. It is notable to mention that spinning one sample with the level code (-1, 1, 0) was impractical because the end breakage rate was very high, which obstructed the spinning process. Therefore a total of 12 yarn samples were spun and tested.

The fibres used and yarns spun were conditioned for 24 hours at 20±2 °C and 65±2% relative humidity prior to testing. The fibre strength and fineness were measured using a Lenzing Vibrodyn-400 (Austria) according to ENISO1973. The fibre length distribution was obtained using a Sinus instrument (England) according to ASTMD1447. SEM analysis was performed to analyse the yarn structure, where samples were coated by gold sputtering for 45s and analysed by means of a yarn longitudinal view using a Carl Zeiss – EVO-LS10 Scanning Electron Microscope (Germany) operated at a voltage of 2 kV. The yarn number of wraps per meter and average helix angle were measured. The yarn diameter was measured using an Uster tester according to ASTM1425 (Switzerland). Yarn strength was measured at a short gauge length (30 mm) using a Labortech instrument according (Czechia) to ASTM D2256. The ordinary least squares regression model was used to analyse the test results and obtain a regression ***Equation (1)***.

Table 1. *Spun yarn production parameters.*

Parameters \ Level codes	-1	0	1
Yarn count, tex	16	23	30
Delivery speed, m/min	350	400	450
Nozzle pressure, bar	4	5	6

$$Y = \beta_0 + \beta_i X_i + \beta_j X_{j+} \beta_k X_k + \beta_{ij} X_i X_j + \\ + \beta_{ij} X_i X_j + \beta_{ik} X_i X_k + \beta_{jk} X_j X_k + \\ + \beta_{ii} X_i{}^2 + \beta_{jj} X_j{}^2 + \beta_{kk} X_k{}^2 \quad (1)$$

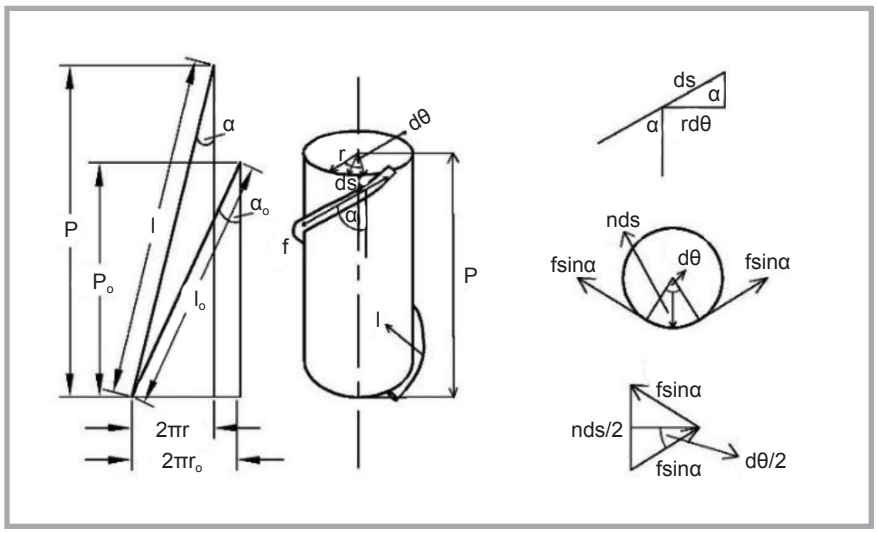

Figure 3. *Force analysis of air jet yarn before and during axial tensile loading (adapted and reproduced [21]).*

Where Y is the dependent variable, X_i, X_j, X_k the independent variables, β_0 the regression equation constant, β_i, β_j, β_k the linear coefficients, β_{ij}, β_{ik}, β_{jk} the interaction coefficients, and β_{ii}, β_{jj}, β_{kk} are the quadratic coefficients.

Derivation of mathematical model

In the current model, the air jet yarn structure has been divided into the core, which is almost parallel fibres, and wrapper, which is in a helical form. The core strand strength has been calculated as a parallel bundle of fibres. This strand is also subjected to the normal forces of the wrapper fibres. Therefore the frictional forces applied to the core fibres strand have been calculated. In addition, the strength of the wrapper fibre strand has also been calculated. It is worth mentioning that the predicted core fibre strand has been calculated based on the assumption that the fibres are gripped between two jaws and the gauge length of the yarn tensile tester is less than the fibre length. Consequently to verify the model, the air jet yarn strength was measured at a gauge length shorter than the fibre length. Given that the irregular nature of the air jet yarn structure originated from the yarn twist, which is inserted pneumatically rather than mechanically as in ring spun yarn, the air jet yarn structure was assumed to be ideal, as shown in ***Figure 2***. The wrap width and height are constant and distributed regularly along the yarn axis; the helix angle is constant, and core fibres are straight and parallel to the yarn axis.

Determination of core fibre strength

There are two components that contribute to core yarn strength: firstly the strength of a parallel bundle of fibres gripped between the two jaws of a tensile testing instrument, and secondly the strength of that bundle originating from a fibre-to-fibre frictional force caused by the normal forces from the wrapper fibre strand during the extension process, assuming that the yarn cross-section is circular and remains so till breaking. To obtain the normal forces on core fibres, Krause et al.'s model was used [21, 22]. By analysing the forces acting on an element of a wrapper fibre, as shown in ***Figure 3***, and following the same derivation steps, ***Equations (2-7)*** have been used to calculate the average strained wrapper fibre helix angle α, the average strained pitch of wrapper fibres p, the strained yarn radius r, and normal forces exerted by wrapper fibres per unit length N.

$$e_y = 2(sin\,\alpha_o)^2 - 1 + \\ + \sqrt{(2(sin\,\alpha_o)^2 - 1)^2 + e_f(2 + e_f)} \quad (2)$$

$$e_r = -e_y \quad (3)$$

$$sin\,\alpha = \left(\frac{1+e_r}{1+e_f}\right) sin\,\alpha_o \quad (4)$$

$$p = p_o(1 + e_y) \quad (5)$$

$$r = r_o(1 + e_r) \quad (6)$$

$$N = \frac{\sigma_f(\sin\alpha)^2}{r} \quad (7)$$

Where e_y expresses the yarn longitudinal strain, α_o the average unstrained wrapper fibre helix angle, e_f the fibre elongation at break, e_r the yarn lateral strain, p_o the average unstrained pitch of wrapper fibres, σ_f the fibre breaking load, and r_o is the unstrained yarn radius.

Therefore the total frictional forces on core fibres σ_1 as a result of the total normal forces exerted by the wrapper fibre strand can be obtained as follows,

$$\sigma_1 = v_f \mu \frac{\sigma_f(\sin\alpha)^2}{r} \frac{W}{100} \frac{T_y}{T_f} p \quad (8)$$

Where, μ is the fibre friction coefficient, T_y yarn linear density, W the wrapper fibre percentage in the yarn, T_f the fibre linear density, and v_f the yarn packing density (assumed constant = 0.6 [25]).

To calculate the other component of core fibre strength, assume a short staple fibre yarn is gripped between tensile tester gauges with a gauge length less than the fibre length. And assuming that these fibres are straight, parallel to the yarn axis, have equal circular diameters, no slippage occurring between core fibres due to the usage of short gauge length, inter-fibre friction so small that it can be ignored, and that the individual fibre position in the yarn is random, then using the Neckář's theory of a parallel fibre bundle [25], the fibre length utilization factor η can be calculated using the following formula,

$$\eta = \begin{cases} \int_0^{l_{max}} \left(1 - \frac{h}{l}\right) \gamma(l)\, dl, & h < l_{max} \\ 0, & h \geq l_{max} \end{cases} \quad (9)$$

Where, h denotes the gauge length, l the fibre length, and $\gamma(l)$ is the mass fraction function, which is the summation of the partial mass fractions of each fibre in the yarn, and can be calculated by analysing the fibre length distribution graph and using the following formula:

$$\gamma(l) = \sum_{j=1}^{k} \frac{m_j}{m} \quad (10)$$

Where, m_j is the mass of the j[th] fibre and m is the mass of the yarn calculated at the maximum fibre length. The value of $\gamma(l)$ ranges from 0 to 1. If all fibres in the yarn have the same length and are equal to the maximum fibre length, then $\gamma(l)$ will be equal to 1 and the parallel bundle strength will be a function of the gauge length only. Thus the core fibre strength as a parallel bundle gripped between two jaws σ_2 can be obtained using ***Equations (9)*** and ***(10)*** as follows,

$$\sigma_2 = \sigma_f \frac{100 - W}{100} \frac{T_y}{T_f} \eta \quad (11)$$

Wrapper fibre strength component

The following assumptions were taken into consideration: (a) a uniform normal pressure exists on core fibres due to the wrapping effect; (b) the wrapping angle is constant, and (c) fibres break simultaneously due to extension at a gauge length less than the fibre length. It is possible to obtain the total wrapper fibre strength σ_3 using the following relation [21].

$$\sigma_3 = \sigma_f \cos\alpha \frac{W}{100}\frac{T_y}{T_f} \qquad (12)$$

According to ***Equations (2-12)***, it is possible to obtain the yarn strength σ_Y as follows:

$$\sigma_Y = \sigma_1 + \sigma_2 + \sigma_3 \qquad (13)$$

The yarn wrapper ratio *W* can be considered as the average volumetric ratio between wrapper fibres and yarn at different yarn sections; thus it can be obtained using the following formula,

$$W = \frac{C(B^2 - A^2)}{C(B^2 - A^2) + A^2 D} \qquad (14)$$

Figure 4 shows a 30 tex yarn longitudinal view under SEM. Random yarn sections were analysed and parameters *A*, *B*, *C* and *D* obtained.

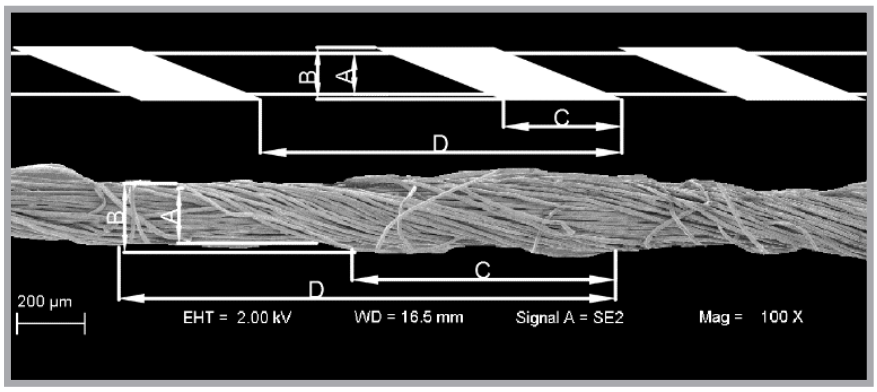

Figure 4. *30 tex viscose yarn longitudinal view under SEM.*

Results and discussion

Table 2 shows the fibre parameters that were obtained and used as an input for the calculation, while ***Table 3*** shows the theoretical and experimental yarn strength values along with its corresponding structural parameters measured under SEM. Results show that the model proposed exhibits good agreement with experimental results of the yarn breaking load, where the prediction error varies from 2-13%. The higher values of prediction error could be ascribed to the variation in the values of wrapper fibre helix angle measured, in the wrapper fibre ratio, and in the number of wraps per unit length. The squared multiple regression coefficient (R^2) along with the regression equations (response surface equations) were estimated for the experimental and theoretical yarn strength as shown in ***Table 4***. All regression coefficients and their P-values are given ***Table 5***.

Table 2. *Viscose fibre properties.*

Fibre friction coefficient, –	0.35
Fibre breaking elongation, %	19.4
Fibre fineness, tex	0.13
Fibre breaking load, cN	3.28

Table 3. *Theoretical and experimental yarn results.* ***Note:*** ** The values in brackets indicate the coefficient of variation (CV%) of the parameter measured.*

Sample	Actual yarn count, tex	Wrapper fibre ratio, %	Yarn diameter, mm	Average unstrained wrapper fibre helix angle, rad	Yarn wraps per meter	Predicted yarn breaking load, cN	Experimental yarn breaking load, cN	Prediction error, %
1	15.9	33.36 (19)	0.20	0.45 (23)	825	224.41	237.85	5.65
2	15.6	28.82 (42)	0.23	0.40 (31)	714	195.42	214.95	9.09
3	16.4	33.25 (18)	0.21	0.45 (19)	700	237.64	241.55	1.62
4	22.4	34.3 (21)	0.24	0.55 (13)	668	347.37	401.99	13.59
5	22.6	31.82 (27)	0.23	0.53 (18)	698	329.07	370.19	11.11
6	22.6	32.85 (28)	0.28	0.51 (22)	635	323.97	372.39	13
7	22.7	37.01 (20)	0.25	0.54 (16)	658	366.74	377.68	2.89
8	22.4	37.74 (15)	0.25	0.55 (15)	685	366.83	404.85	9.39
9	29.4	37.14 (18)	0.27	0.59 (17)	629	490.97	552.92	11.2
10	29.4	39.42 (9)	0.29	0.61 (18)	562	525.39	551.58	4.75
11	29.5	35.96 (18)	0.29	0.62 (19)	545	502.52	522.89	3.89
12	29.4	36.4 (21)	0.27	0.64 (10)	619	502.49	562.38	10.65

Table 4. *Response surface equations for yarn properties tested.* ***Note:*** **X_1: yarn count, tex, X_2: yarn delivery speed, m/min, X_3: nozzle pressure, bar.*

Dependant variable	Response surface equation	R^2, %
Experimental strength, cN	$-821.9 + 22.4X_1 + 2.4X_2 + 94.4X_3 - 0.2X_1^2 - 0.01X_2^2 - 19.2X_3^2 + 0.01X_1X_2 + 1.4X_1X_3 + 0.2X_2X_3$	95.5
Theoretical strength, cN	$-569.5 + 8.3X_1 + 1.8X_2 + 81.9X_3 + 0.07X_1^2 - 0.005X_2^2 - 17.4X_3^2 + 0.04X_1X_2 + 0.9X_1X_3 + 0.3X_2X_3$	98

Table 5. *P-values of the experimental strength model and its coefficients.* ***Note:*** **Statistically significant at 95% confidence level.*

Coefficient	β_0	β_i	β_j	β_k	β_{ij}	β_{ik}	β_{jk}	β_{ii}	β_{jj}	β_{kk}	Regression model F, P-value
P-value	0.01*	0.00*	0.00*	0.02*	0.01*	0.04*	0.00*	0.00*	0.00*	0.03*	0.02*

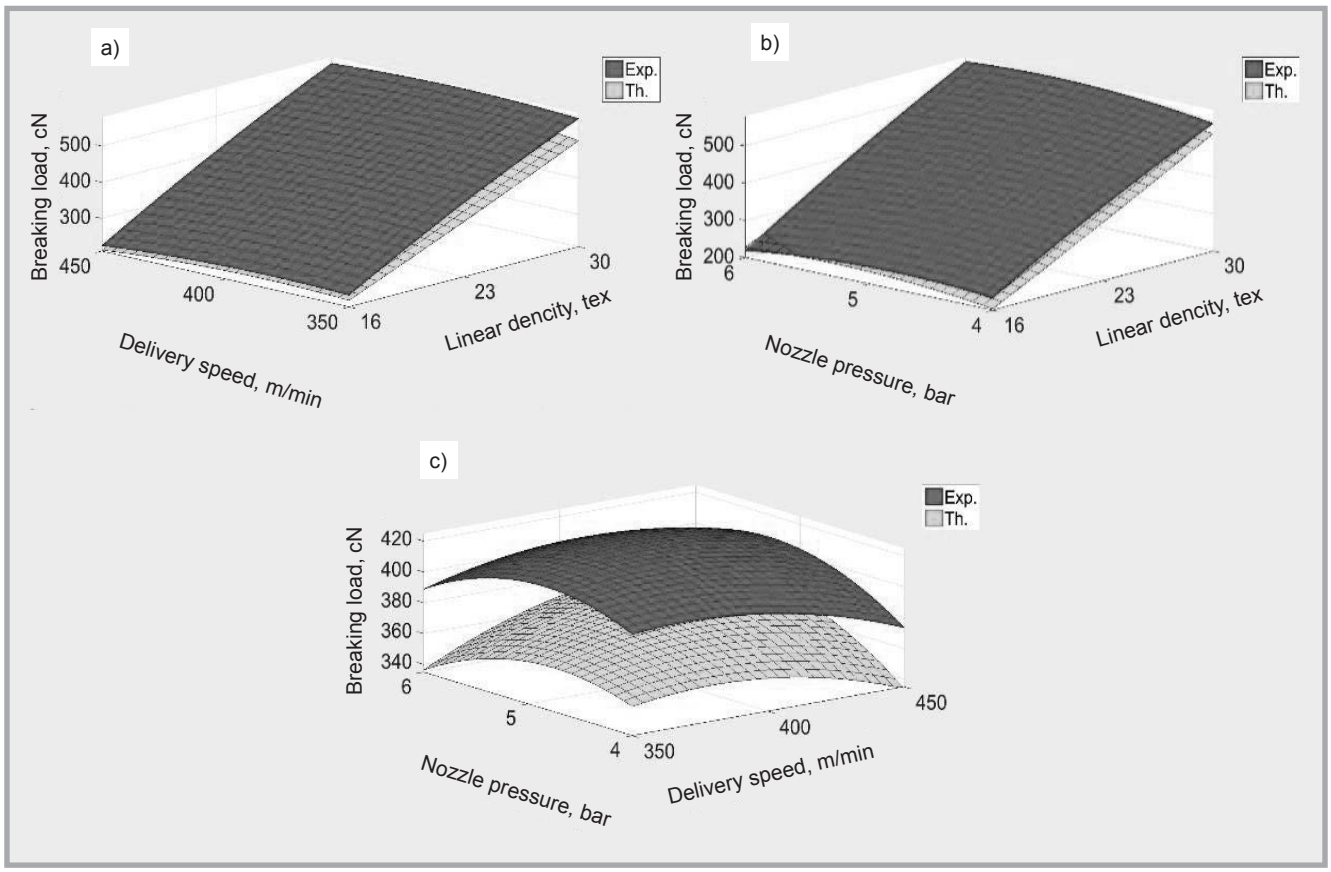

Figure 5. *Combined effect of a) yarn linear density and delivery speed, b) yarn linear density and nozzle pressure, and c) nozzle pressure and delivery speed on yarn strength.*

Figures 5 shows the influence of the linear density, delivery speed and nozzle pressure on yarn strength. The analysis of variance showed that the differences in yarn strength are statistically significant at a 95% confidence level. It is obvious that the linear density has the maximum effect on yarn strength. As shown in ***Figure 5.a***, ***5.b***), coarser yarns of 30 tex have higher strength than finer yarns of 16 tex, due to the increase in the number of fibres in the yarn cross-section, thus the existence of a higher proportion of core fibres that bear the load exerted on the yarn. The same trend also exists in MVS yarn [10].

Figure 5.c shows that increasing the yarn delivery speed from 350 to 400 m/min results in increasing the yarn strength, particularly at 6 bar; but when using a high delivery speed of 450 m/min, a deterioration in yarn strength of about 7% occurs, which is a consequence of the insufficient time for the whirling action to take place in the vortex chamber, resulting in an increment in the number of wild fibres and regions of unwrapped core fibres [26].

Also from ***Figure 5.c***, it is observed that the yarn strength increases when the nozzle pressure increases from 4 to 5 bar, and then decreases gradually when it reaches 6 bar, because the rise in air pressure initially causes tight regular wrappings and more wrapped portions of the yarn; but higher air pressure creates irregular wrappings and increases the wild fibres. The same trend is also confirmed for MVS yarn [10]. However, it should be noted that unlike fine yarns, when using the high pressure of 6 bar, the strength of coarse yarns did not change (***Figure 5.b***). By observing the trend of the theoretical and experimental values of yarn strength in ***Figure 5***, it can be concluded that the mathematical model captures the change in yarn strength well as the yarn linear density, delivery speed and nozzle pressure change.

Conslusions

This study focuses on the effect of yarn count, nozzle pressure and delivery speed on Rieter air jet spun yarn strength. It is clear that coarser counts have a higher tensile strength. Increasing the nozzle pressure results in increasing tight regular wrappings and more wrapped portions, and consequently the yarn strength increases initially, but later on it decreases at higher pressures because of the incidence of irregular wrappings, and an increase in wild fibres and fibre loss. Using high delivery speeds deteriorates the yarn tensile strength because of the insufficient time for the whirling action to take place in the vortex chamber, which results in an increment in the number of wild fibres as well as the regions of unwrapped core fibres. Response surface equations showed that the yarn count range taken (16-30 tex) has the maximum effect on yarn tensile strength. Moreover maximum tensile strength values (greater than 522 N) are obtained at coarser counts (30 tex). For seeking the optimal machine setting it is suggested to adjust the delivery speed within the range of 350 to 400 m/min and nozzle pressure to 5 bar for the whole range of yarn linear density. These settings are similar to the optimal running conditions of the MVS to a great extent. The general trend of the influence of the parameters studied on the Rieter air jet yarn strength was found to be similar to its corresponding MVS yarn.

Based on fibre parameters and air jet spun yarn structural parameters, it is possible to predict the air jet yarn strength at a short gauge length using the model presented in this article. The model calculated three components of strength: the core strength as a parallel bundle of fibres, the wrapper fibre pressure on core fibres, and the wrapper fibre strength. The model may be developed to calculate the yarn strength at a longer gauge length (500 mm).

References

1. Kostajnšek K, Dimitrovski K. Comparative Study on the Properties of Vortex and Ring Spun Yarn and the Properties of Woven Fabrics Containing Those Yarns in Weft. *FIBRES & TEXTILES in Eastern Europe* 2016; 24, 2(116): 59-65. DOI: 10.5604/12303666.1191428.
2. Zou Z. Study of the stress relaxation property of vortex spun yarn in comparison with air-jet spun yarn and ring spun yarn. *FIBRES & TEXTILES in Eastern Europe* 2012; 20, 1(90): 28-32.
3. Erdumlu N, Ozipek B, Oxenham W. Vortex spinning technology. Text. Prog. 2012; 44, 3-4: 141-174.
4. United States Patent and Trademark Office. US Patent 2007/0125062 A1, http://www.uspto.gov," 2007.
5. Erdumlu N, Ozipek B. Effect of the draft ratio on the properties of vortex spun yarn. *FIBRES & TEXTILES in Eastern Europe* 2010; 80, 3: 38-42.
6. Basal G. Effects of some process parameters on the structure and properties of vortex spun yarn. *Text. Res. J.* 2006; 76, 6: 492-499.
7. Erdumlu N, Oxenham W, Ozipek B. The impact of combing and processing parameters on the structure and properties of fine count vortex yarns. *Text. Res. J.* 2013; 83, 4: 396-405.
8. Gordon S. The effect of short fibre and nep levels on Murata vortex spinning efficiency and product quality. Final Rep. To CanC, CSIRO *Text. Fibre Technol.* 2001; October: 1-14.
9. Zou Z Y. Influence of the Yarn Formation Process on the Characteristics of Viscose Fabric Made of Vortex Coloured Spun Yarns. *FIBRES & TEXTILES in Eastern Europe* 2015, 23, 3(111): 58-63. DOI: 10.5604/12303666.1152467.
10. Rajamanickam R, Hansen S M, Jayaraman S. Studies on fiber–process–structure–property relationships in air-jet spinning. part II: model development. *J. Text. Inst.* 1998; 89, 2: 243-265.
11. Ortlek H G. Effect of some variables on properties of 100% cotton vortex spun yarn. Text. Res. J. 2005; 75, 6: 458-461.
12. Ortlek H G, Nair F, Kilik R, Guven K. Effect of spindle diameter and spindle working period on the properties of 100% viscose MVS yarns. *FIBRES & TEXTILES in Eastern Europe* 2008; 16, 3: 17-20.
13. Johnson W M. *The impact of MVS machine settings and finishing applications on yarn quality and knitted fabric hand*. MSc Thesis, Institute of Textile Technology, Charlottesville, Virginia, USA, 2002.
14. Sharma D. Performance and low-stress characteristics of polyester-cotton MVS yarns. *Indian J. Fibre Text. Res.* 2004; 29, September: 301-307.
15. Onder E, Baser G. A comprehensive stress and breakage analysis of staple fiber yarns, part I: stress analysis of a staple yarn based on a yarn geometry of conical helix fiber paths. *Text. Res. J.* 1996; 66, 10: 634-640.
16. Zurek W, Frydrych I, Zakrzewksi S. A method of predicting the strength and breaking strain of cotton yarn. *Text. Res. J.* 1987; 57, 8: 439-444.
17. -Ning P. Development of a constitutive theory for short fiber yarns, part II: mechanics of staple yarn with slippage effect. *Text. Res. J.* 1993; 63, 9: 504-514.
18. Aggarwal S K. A model to estimate the breaking elongation of high twist ring spun cotton yarns, part I: derivation of the model for yarns from single cotton varieties. *Text. Res. J.* 1989; 59, 11: 691-695.
19. Zubair M, Neckář B, Malik Z A. Predicting Specific Stress of Cotton Staple Ring Spun Yarns: Experimental and Theoretical Results. *FIBRES & TEXTILES in Eastern Europe* 2017; 25, 2(122): 43-47. DOI: 10.5604/12303666.1228166.
20. Jiang X Y, Hu J L, Postle R. A new tensile model for rotor spun yarns. *Text. Res. J.* 2002; 72, 10: 892-898.
21. Krause H W, Soliman H A. Theoretical study of the strength of single jet false twist spun yarns. *Text. Res. J.* 1990; 60, 6: 309-318.
22. Xie Y, Oxenham W, Grosberg P. 25 – A study of the strength of wrapped yarns, part II: computation and experimental. *J. Text. Inst.* 1986; 77, 5: 305-313.
23. Rajamanickam R, Hansen S M, Jayaraman S. Analysis of the modeling methodologies for predicting the strength of air-jet spun yarns. *Text. Res. J.* 1997; 67, 1: 39-44.
24. Rajamanickam R, Hansen S M, Jayaraman S. A model for the tensile fracture behavior of air-jet spun yarns. *Text. Res. J.* 1998; 68, 9: 654-662.
25. Neckar and B, Das D. A stochastic approach to yarn strength, in Seventh Asian Textile Conference, 2003.
26. Tyagi G K, Sharma D, Salhotra K R. Process-structure-property relationship of polyester-cotton MVS yarns, part I: influence of processing variables on yarn structural parameters. *Indian J. Fibre Text. Res.* 2004; 29, 4: 419-428.

Received 10.02.2017 Reviewed 13.11.2017